RESEARCH ARTICLE | OCTOBER 14 2014

Dynamics of the OH group and the electronic structure of liquid alcohols

Simon Schreck; Annette Pietzsch; Kristjan Kunnus; Brian Kennedy; Wilson Quevedo; Piter S. Miedema; Philippe Wernet; Alexander Föhlisch

Struct. Dyn. 1, 054901 (2014)
https://doi.org/10.1063/1.4897981

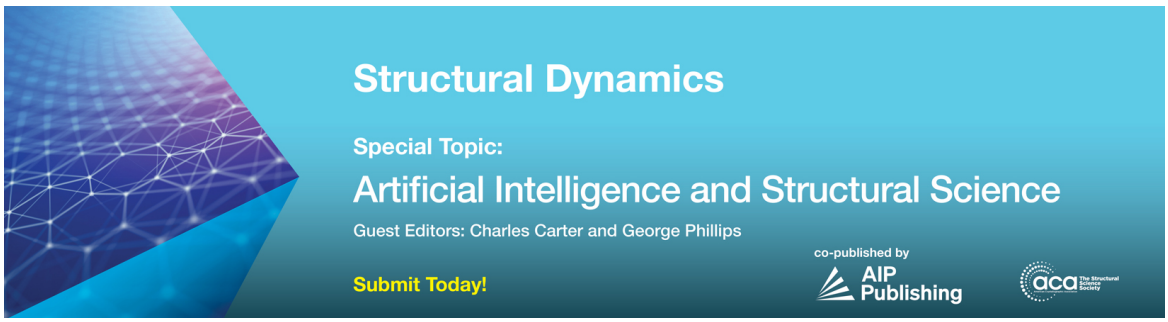

Dynamics of the OH group and the electronic structure of liquid alcohols

Simon Schreck,[1,2,a)] Annette Pietzsch,[1] Kristjan Kunnus,[1,2] Brian Kennedy,[1] Wilson Quevedo,[1] Piter S. Miedema,[1] Philippe Wernet,[1] and Alexander Föhlisch[1,2,b)]
[1]*Institute for Methods and Instrumentation for Synchrotron Radiation Research, Helmholtz-Zentrum Berlin für Materialien und Energie GmbH, Albert-Einstein-Strasse 15, Berlin 12489, Germany*
[2]*Institut für Physik und Astronomie, Universität Potsdam, Karl-Liebknecht-Strasse 24/25, Potsdam 14476, Germany*

(Received 11 July 2014; accepted 30 September 2014; published online 14 October 2014)

In resonant inelastic soft x-ray scattering (RIXS) from molecular and liquid systems, the interplay of ground state structural and core-excited state dynamical contributions leads to complex spectral shapes that partially allow for ambiguous interpretations. In this work, we dissect these contributions in oxygen K-edge RIXS from liquid alcohols. We use the scattering into the electronic ground state as an accurate measure of nuclear dynamics in the intermediate core-excited state of the RIXS process. We determine the characteristic time in the core-excited state until nuclear dynamics give a measurable contribution to the RIXS spectral profiles to $\tau_{dyn} = 1.2 \pm 0.8$ fs. By detuning the excitation energy below the absorption resonance we reduce the effective scattering time below τ_{dyn}, and hence suppress these dynamical contributions to a minimum. From the corresponding RIXS spectra of liquid methanol, we retrieve the "dynamic-free" density of states and find that it is described solely by the electronic states of the free methanol molecule. From this and from the comparison of normal and deuterated methanol, we conclude that the split peak structure found in the lone-pair emission region at non-resonant excitation originates from dynamics in the O–H bond in the core-excited state. We find no evidence that this split peak feature is a signature of distinct ground state structural complexes in liquid methanol. However, we demonstrate how changes in the hydrogen bond coordination within the series of linear alcohols from methanol to hexanol affect the split peak structure in the liquid alcohols. [http://dx.doi.org/10.1063/1.4897981]

I. INTRODUCTION

Soft x-ray spectroscopies are well-established electronic structure tools. Their ability to probe local charge distributions in an element specific and symmetry resolved manner has been demonstrated and exploited in numerous studies of molecules, solids, and surfaces to reveal their structure and bonding as well as the dynamics of elementary chemical processes.[1–3] In the past decade, soft x-ray spectroscopies, furthermore, have been used increasingly to study the structure of complex molecular and liquid systems. In particular, the fluctuating hydrogen bond network in liquid water was investigated intensively.[4–15]

In x-ray emission (XE) spectroscopy and resonant inelastic x-ray scattering (RIXS) at the oxygen K-edge of liquid water, a debate about ground state structural and core-excited state dynamical contributions to the measured spectra is ongoing.[11,12,14,16,17] In particular, the origin of

[a)]Electronic mail: simon.schreck@helmholtz-berlin.de
[b)]Electronic mail: alexander.foehlisch@helmholtz-berlin.de

a splitting in the region of the $1b_1$ lone-pair derived emission feature is controversially discussed. On one hand, the two split components have been assigned to two distinct structural motifs, denoted as high and low density liquid water, which coexist in the liquid phase. In this picture, the splitting is primarily an intrinsic ground state feature of liquid water and originates from an energy shift of the oxygen 1*s* core level between the two structural motifs.[11,14] Here, contributions from nuclear dynamics in the intermediate core-excited state of the RIXS process are found to mainly cause an asymmetric broadening of the lone-pair emission line.[18] On the other hand, the splitting was interpreted fully as a dynamical effect resulting from nuclear motion in the intermediate state.[12,16,17] In this picture, the splitting is not a ground state property of liquid water but induced by the core level excitation. Both interpretations have been supported and challenged[18–23] and no consensus seems to be found.

In this debate, surprisingly less attention has been given to the liquid alcohols, which also show a splitting in the lone-pair region of the oxygen K-edge RIXS spectra.[24–27] So far, Kashtanov *et al.*[26] performed the most detailed RIXS study of liquid methanol. With the help of density functional theory calculations they assigned the two split components in the lone-pair region to hydrogen bonded rings and chains, respectively, with a length of six or eight molecules, which should dominate the structure of liquid methanol. Recent high-level molecular dynamics simulations[28,29] are at variance with this interpretation, and suggest that liquid methanol consists mainly of hydrogen bonded chains with less than seven molecules, which may link to branched aggregates. The core-excited state dynamical contributions in RIXS from liquid alcohols have so far not been studied in detail.

In this work, we dissect the ground state structural and core-excited state dynamical contributions in RIXS from liquid alcohols. We present experimental RIXS spectra of liquid methanol in its normal (CH_3OH) as well as in its deuterated form (CD_3OD) and analyze the spectral changes as the excitation energy is tuned below the absorption resonance. The concept of effective scattering time[30] enables us to control the degree of nuclear dynamics in the intermediate core-excited state of the RIXS process. The vibrational progression of elastic scattering into the electronic ground state (participator decay) serves as an "internal clock" to measure the degree of nuclear dynamics. We determine the characteristic time in the core-excited state until nuclear dynamics have a measurable contribution to the RIXS spectral profiles for liquid methanol. We use an approximation to the generalized Kramers-Heisenberg scattering formalism to model the strongly detuned RIXS spectra, where nuclear dynamics in the intermediate state is suppressed to a minimum. This way we are able to extract the "dynamic-free" local partial density of states (DOS) of liquid methanol and find that it is fully described by the electronic states of the free methanol molecule. From the comparison of normal and deuterated methanol, we find evidence that the split peak structure in the liquid alcohols originates from dynamics in the O–H bond in the core-excited state. We propose a mechanism based on qualitative potential energy curves of the hydrogen bond donating OH group that explains the formation of the split peak structure. In the series of the liquid alcohols from methanol to hexanol the hydrogen bond environment gradually changes and we show how this affects the split peak structure.

II. EXPERIMENTAL

The experimental procedures are depicted schematically in Figure 1(a). We recorded the x-ray absorption (XA) spectrum of liquid methanol in transmission mode using the specialized sample holder described by Schreck *et al.*[31] The measurements were performed at the dipole beamline PM3 at the synchrotron radiation source BESSY II of the Helmholtz-Zentrum Berlin.

We measured RIXS spectra from a liquid microjet in vacuum using the setup described by Kunnus *et al.*[32] The setup uses a Grace XES 350 x-ray emission spectrometer, which is mounted under 90° with respect to the incident x-ray beam, Figure 1(a). We used linearly polarized x-rays with the polarization vector in the scattering plane. In addition, we used this setup to measure total fluorescence yield (TFY) XA spectra from the liquid jet with a GaAsP photodiode (Hamamatsu, model G-112704) for the alcohols from methanol to hexanol. The

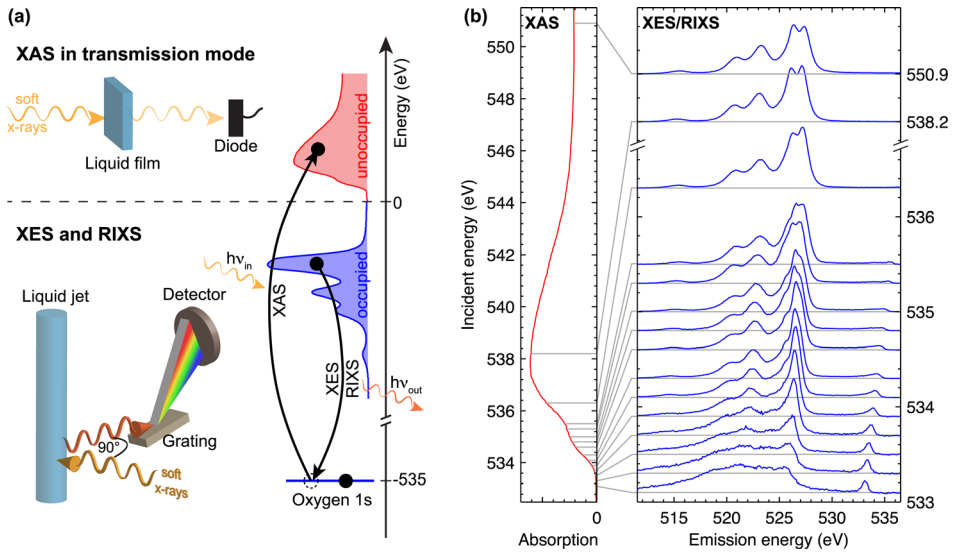

FIG. 1. X-ray absorption and emission spectroscopy (XAS and XES) as well as RIXS from liquid methanol: (a) Illustration of the experimental procedures for XAS in transmission mode and XES/RIXS from a liquid jet. The simplified energy scheme shows how in the one electron picture XAS and XES/RIXS probe the unoccupied and occupied DOS. (b) Experimental XA spectrum of liquid methanol (CH_3OH) together with the corresponding RIXS spectra for excitation energies tuned through the XA resonance. The RIXS spectra are offset by their respective excitation energy. Grey lines indicate the excitation energies in the XA spectrum.

measurements were performed at beamlines U41-PGM and UE52-SGM at the synchrotron radiation source BESSY II of the Helmholtz-Zentrum Berlin.

For energy calibration of the incident x-ray beam in the RIXS measurements we used the sharp π^* XA peak of liquid acetone at 531.5 eV.[27] We calibrated the emission energy scale using the elastically scattered light. The energy scale of the transmission mode XA spectrum was aligned by overlapping it with the TFY XA spectrum of liquid methanol, which was recorded in the same experimental run as the RIXS measurements.

Samples were purchased from Sigma-Aldrich, had a purity of 99.5% or higher and were used as received. Deuterated methanol was handled in nitrogen atmosphere only.

III. RESULTS

A. XA and RIXS spectra from liquid methanol

In Figure 1(b), we present an overview of the experimental data from liquid methanol (CH_3OH). The oxygen K-edge XA spectrum measured in transmission mode is presented together with respective RIXS spectra for excitation energies tuned through the XA resonance.

The XA spectrum features a broad resonance between 534 and 544 eV with a maximum at around 538 eV and a weak shoulder on the low energy flank around 535 eV. The shoulder originates from the O–H anti-bonding σ^* orbital, as was established by density functional theory calculations and comparison to gas phase data.[33] In the broad absorption maximum, the C–O σ^* orbital as well as 3*p* type Rydberg states overlap.[33]

The RIXS spectra in Figure 1(b) agree with previously published data.[24–26] However, the data presented here exhibit significantly increased signal-to-noise ratio, a slightly enhanced spectral resolution as well as a broader range of excitation energies as compared to all publications that are known to the authors.

The non-resonant XE spectrum at 550.9 eV excitation energy features three well-separated emission lines at around 515, 521, and 523 eV emission energy as well as the split peak structure mentioned in the introduction at around 527 eV emission energy.

As the incident photon energy is tuned to resonant excitations and consequently detuned below resonance, the main changes in the RIXS spectra occur in the split peak structure. This

structure collapses into a single peak and at the same time reveals a shoulder on its low energy flank around 525.5 eV (see also Figure 2(b)). After close inspection, this weak shoulder can also be identified in the non-resonant spectrum. All emission features undergo Raman dispersion, as the excitation energy is tuned below resonance. For strongly detuned excitation energies (below 533.3 eV) the emission lines get significantly broadened and the RIXS spectra turn into one broad feature with weak substructure. We analyze this effect in detail in Sec. III C.

We observe elastic scattering, where the emission energy equals the excitation energy, for incident photon energies below 536.3 eV. For higher excitation energies, the probability for the excited electron to fill the core hole gets relatively small and we detect no elastic scattering (not shown in Figure 1(b)). For the lowest excitation energies, the elastic peak is symmetric, whereas it develops a low energy tail for higher excitation energies. This low energy tail is related to nuclear dynamics in the intermediate state of the RIXS process, and we analyze this in detail in Sec. III B.

B. Vibrational progression as a measure for nuclear dynamics in the core-excited state

We now concentrate on excitation energies in the low energy flank of the XA resonance between 533.1 and 536.3 eV, where the major changes in the RIXS spectra occur. In Figure 2, we present a zoom into the corresponding region of the XA spectrum (Figure 2(a)), the split peak emission feature (Figure 2(b)) as well as the elastic scattering (Figure 2(c)).

We subdivide the spectral intensity around the elastic scattering (Figure 2(c)) into contributions from three distinctly different decay processes of the core-excited state. These decay processes are depicted schematically in Figure 2(e). First, the high-energy tail of decay into electronic valence-excited states extends into the region of elastic scattering (light blue area in Figure 2(c)). We model this intensity by interpolation between the high energy flank of the split peak feature and the zero intensity at emission energies higher than the excitation energy.[34] Second, there is purely elastic scattering at zero energy loss (green area in Figure 2(c)), which corresponds to decay into the vibrational and electronic ground state. This intensity is modeled by fitting a symmetric Gaussian peak centered at zero energy loss to the high energy flank of the elastic scattering. The remaining spectral intensity (orange area in Figure 2(c)) corresponds

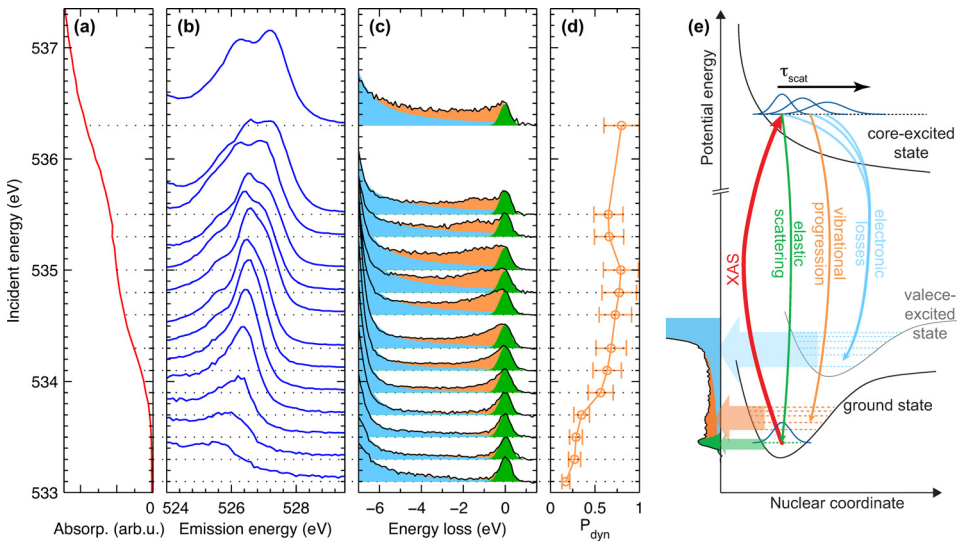

FIG. 2. Excitation energy detuning and control of nuclear dynamics in RIXS. (a) Low energy flank of the XA resonance. (b) Split peak emission feature of the RIXS spectra excited in the XA flank and below the resonance. (c) Region of elastic scattering for excitation in the XA flank and below the resonance. The spectral intensity is subdivided into the three decay channels from the core-excited state, which are depicted in (e) of the figure. See main text for details. The experimental data in (a)-(c) are the same as in Figure 1. (d) Probability for nuclear dynamics in the core-excited state as determined from the intensities in (c). See main text for details. (e) Schematic illustration of how nuclear dynamics are manifested in the vibrational progression.

to decay into vibrational excited states of the electronic ground state, the vibrational progression. At very high spectral resolution, individual vibrational states are observed in the progression also for liquid systems.[15,27,35] This is not the case in the present study. However, we observe a significant decrease of intensity in the progression when the excitation energy is detuned below the absorption resonance.

The vibrational progression and its collapse for detuned excitation energies are connected to nuclear dynamics in the intermediate core-excited state of the RIXS process and to the concept of the effective scattering time of RIXS.[30,36,37] In a quantum mechanical picture, nuclear dynamics in the intermediate state correspond to the propagation of the nuclear wave packet on the core-excited state potential. The XA process projects the electronic and vibrational ground state nuclear wave packet onto the core-excited state potential (Figure 2(e)). The ground state wave packet will propagate on the excited state potential, since it is, in general, not an Eigenstate of this potential. The propagated wave packet reaches Franck-Condon overlap with vibrational excited states of the electronic ground state, and hence decay into these vibrational excited states is possible. This gives rise to the vibrational progression. On the other hand, the purely elastic scattering corresponds to the case, where the nuclear wave packet has not propagated significantly on the excited state potential. That is, it results from decays immediately after the XA process.

The concept of effective scattering time determines for Raman-type scattering processes, like RIXS, the time the system spends in the intermediate state. This time shortens upon detuning the excitation energy from the scattering resonance and is given by[30]

$$\tau_{\mathrm{scat}} = \frac{1}{\sqrt{\Omega^2 + \Gamma_{\mathrm{ch}}^2}}. \tag{1}$$

Here, Ω is the detuning and Γ_{ch} is the core level lifetime broadening, which is directly connected to the natural core hole lifetime $\tau_{\mathrm{ch}} = 1/\Gamma_{\mathrm{ch}}$. Atomic units are used. The oxygen $1s$ core hole lifetime is $\sim$4 fs.[38]

For a shortened effective scattering time, the nuclear wave packet has less time to propagate on the excited state potential, and hence reaches overlap with less vibrational excited states of the electronic ground state; the vibrational progression collapses.

We now use the relative intensity of the vibrational progression as a measure for the degree of nuclear dynamics in the core-excited state. We define the probability P_{dyn} that the core-excited state decays after significant nuclear dynamics give rise to vibrational progression in the spectra. This probability can be determined from the experimental data in Figure 2(c) for each excitation energy

$$P_{\mathrm{dyn}} = \frac{A_{\mathrm{vib}}}{A_{\mathrm{vib}} + A_{\mathrm{elast}}}. \tag{2}$$

A_{vib} corresponds to the spectral intensity of the vibrational progression (orange area in Figure 2(c)) and A_{elast} to the elastic scattering (green area in Figure 2(c)).

We depict P_{dyn} as a function of the excitation energy in Figure 2(d). Comparing the trend of P_{dyn} to the evolution of the split peak structure in Figure 2(b), we find that the splitting starts to appear at excitation energies, where also P_{dyn} gets significant. This is a first indicator that the split peak structure in liquid methanol is related to nuclear dynamics in the intermediate core-excited state of the RIXS process.

Within a "core hole clock"[39–41] type of approach, we can now retrieve the characteristic time τ_{dyn} until dynamics in the core-excited state have a measurable impact on the RIXS spectral profiles. For simplicity, we assume an exponential rate $\Gamma_{\mathrm{dyn}} = 1/\tau_{\mathrm{dyn}}$ that describes nuclear dynamics in the excited state. This is a good approximation as long as τ_{dyn} and τ_{scat} are on the same order of magnitude (see Brühwiler *et al.*[41] as well as references therein for a detailed discussion). P_{dyn} is connected to Γ_{dyn} and to the scattering rate (core hole decay) $\Gamma_{\mathrm{scat}} = 1/\tau_{\mathrm{scat}}$ by

$$P_{\mathrm{dyn}} = \frac{\Gamma_{\mathrm{dyn}}}{\Gamma_{\mathrm{scat}} + \Gamma_{\mathrm{dyn}}}. \tag{3}$$

The scattering rate Γ_{scat} depends on the detuning Ω (Eq. (1)) and hence on the excitation energy with respect to the resonance energy. A precise definition of the position of the lowest scattering resonance is difficult for the broad XA spectrum in liquid methanol. However, the resonance will be slightly below 535 eV close to the shoulder on the XA flank. For these excitation energies, P_{dyn} has its maximum and is almost constant. For an isolated scattering resonance, P_{dyn} should peak at the resonance position. We determine $\tau_{\mathrm{dyn}} = 1.2 \pm 0.8$ fs (see also Ref. 34) using a scattering rate on resonance of $\Gamma_{\mathrm{scat}} = 1/4\ \mathrm{fs}^{-1}$ and an averaged value for P_{dyn} from excitation energies around the resonance position (534.6, 534.8, and 535.0 eV). The relatively big uncertainty in τ_{dyn} can be reduced by higher signal-to-noise ratio as well as by higher spectral resolution. Resolving single vibrational peaks in the vibrational progression would, e.g., allow for a more accurate separation of purely elastic scattering and the vibrational progression.

We note that τ_{dyn} should not be associated with a dissociation time that characterizes the breaking of a molecular bond. It rather quantifies the time after which nuclear dynamics in the core-excited state have a measurable contribution to the RIXS spectral profiles. In that sense, τ_{dyn} may decrease for higher spectral resolution, but the value determined here provides an upper limit. Dissociation times were determined by other groups[40,42] for different molecular systems from Auger electron spectroscopy using a similar approach.

C. "Dynamic-free" DOS of liquid methanol

For a detuning of $\Omega \approx 1.5$ eV, which corresponds to the lowest excitation energy used in this work (533.1 eV), the effective scattering time is reduced to 0.2 fs. At this excitation energy contributions from nuclear dynamics in the intermediate state are basically absent, which can be seen directly from the absence of the orange shaded intensity in the corresponding spectrum in Figure 2(c). Furthermore, the selectivity in the excitation process is lost at such detuned excitation energies, since the excitation is into the Lorentzian tails of all excited states with almost the same probability.[43] This clears out resonance effects such as the enhancement of particular chemical species. Accordingly, the strongly detuned RIXS spectra should give the best (free of effects from nuclear dynamics and resonant excitation) measure of the local partial (oxygen *p*-type) occupied DOS. However, a direct detailed analysis of these spectra is hindered due to the broadening introduced at detuned excitation energies. This broadening has been observed before in different systems and the corresponding spectra can be modeled by

$$I_{\mathrm{RIXS}}(E_{\mathrm{in}}, E_{\mathrm{out}}) \propto \int_0^{E_{\mathrm{loss}}} \mathrm{d}E_{\mathrm{e}} \frac{\rho_{\mathrm{u}}(E_{\mathrm{e}})\rho_{\mathrm{o}}(E_{\mathrm{loss}} - E_{\mathrm{e}})}{(\Omega - E_{\mathrm{e}})^2 + \left(\frac{\Gamma_{\mathrm{ch}}}{2}\right)^2}. \tag{4}$$

This formula is based on the generalized Kramers-Heisenberg scattering formalism introduced by Tulkki and Åberg.[44,45] Jiménez-Mier *et al.*[46] followed an approach from Cowan[47] and were the first who presented Eq. (4) in the form used here. Other groups used a Green's function approach[48] or considered energy conservation in the scattering process[49] to develop a very similar expression.

In Eq. (4), E_{in} and E_{out} are the energy of the incident (excitation) and outgoing (emission) photon. The integration is over all possible energies E_{e} of the excited electron in the intermediate state, which can take values between zero and $E_{\mathrm{loss}} = E_{\mathrm{in}} - E_{\mathrm{out}}$. Ω is the detuning of the incident energy from the resonance energy E_{res}: $\Omega = E_{\mathrm{in}} - E_{\mathrm{res}}$. Γ_{ch} is the natural core level lifetime broadening. The spectral shape resulting from Eq. (4) is mostly determined by the occupied (ρ_{o}) and unoccupied (ρ_{u}) local partial DOS and the detuning Ω. For excitation energies below resonance ($\Omega < 0$), the Lorentzian in Eq. (4) has its maximum at negative E_{e}, i.e., outside the integration boundaries. For strong detuning ($\Omega \ll -\Gamma_{\mathrm{ch}}$) only the Lorentzian tail is

included in the integration, and Eq. (4) turns into a convolution of occupied and unoccupied DOS.

In the hard x-ray regime, the approach from Tulkki and Åberg[44,45] is used as an established technique to retrieve (single shot) XA spectra from detuned RIXS spectra for, e.g., time resolved XA spectroscopy.[50–53] In the soft x-ray regime, the model was applied to describe RIXS spectra of metals excited above and below threshold.[43,49,54]

We will use Eq. (4) to retrieve the "dynamic-free" occupied DOS from the RIXS spectra at strong detuning. For this, we approximate the unoccupied DOS ρ_u by the measured XA spectrum. To account for the core hole induced shift of the XA spectrum, we align ρ_o and ρ_u relative to each other.[34] For the comparably broad and featureless XA spectrum of liquid methanol core hole induced effects should mainly cause an energy shift and affect the shape of the spectrum marginally.[1,55]

To model the occupied DOS ρ_o, we use a sum of five peaks with pseudo-Voigt profiles. This five peak approach is motivated by the calculated non-resonant XE spectrum of the free methanol molecule (Figure 3(a), dark green line), which shows five peaks corresponding to the occupied valence orbitals of the methanol molecule in C_S symmetry $4a'$, $5a'$, $1a''$, $6a'$, $7a'$, and $2a''$, where the $1a''$ and $6a'$ orbital are energetically almost fully degenerate and hence form one peak.[34,43] Details on the spectrum calculation can be found in the supplementary material.[34] We fit the result of Eq. (4) to the experimental spectrum at 533.1 eV excitation energy by numerically optimizing the peak amplitudes in our model for ρ_o. The peak positions and widths are approximated from the measured non-resonant XE spectrum. The resulting occupied DOS $\rho_{o,\,fit}$ is depicted in Figure 3(a) together with the calculated non-resonant spectrum of the methanol molecule as well as with the experimental non-resonant spectrum of the liquid.

We compare the fitted spectrum ($\rho_o = \rho_{o,\,fit}$) to the experimental data in Figure 3(b). Here, we also include the result of Eq. (4) when using the experimental non-resonant XE spectrum for ρ_o. The fitted spectrum reproduces the broadening as well as the weak substructure in the experimental spectrum well. Minor deviations are present around 519 and above 526.5 eV emission energy. In contrast, the spectrum resulting from the non-resonant XE spectrum for ρ_o shows major deviations in particular in the spectral region that develops into the split peak structure for higher excitation energies. The latter mismatch is a manifestation of nuclear dynamics in the core-excited state, which are present in the non-resonant XE spectrum used for

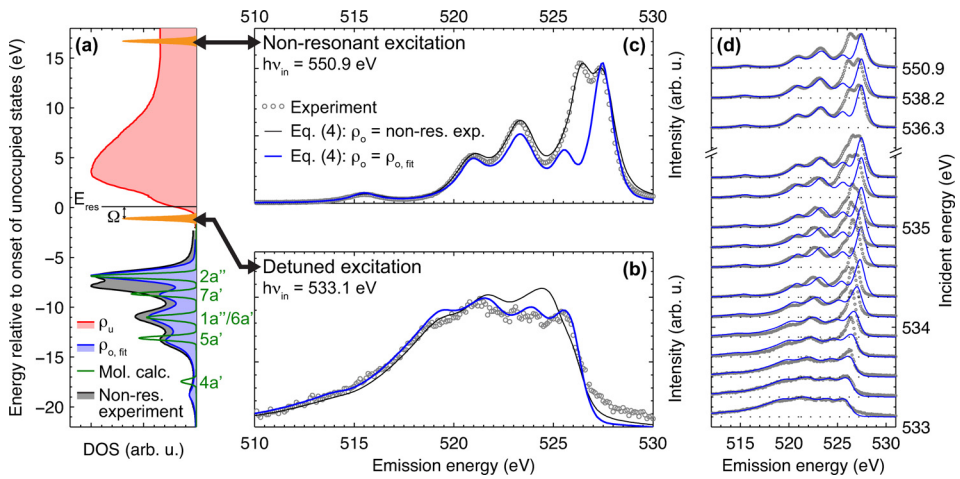

FIG. 3. Retrieving the "dynamic-free" DOS of liquid methanol. (a) Unoccupied DOS and the two models for the occupied DOS as well as the calculated electronic states of the free methanol molecule on an energy scale relative to the onset of the unoccupied states as used for application of Eq. (4). The orange Lorentzian peaks indicate the excitation energies used for detuned (b) and non-resonant (c) excitation. (b) Experimental RIXS spectrum of liquid methanol at detuned excitation together with the fitted spectrum resulting from Eq. (4) with $\rho_o = \rho_{o,\,fit}$ as well the result of Eq. (4) when using the non-resonant XE spectrum for ρ_o. See (c) for the legend. (c) Same as (b) but for non-resonant excitation. (d) Comparison of experimental spectra and the results of Eq. (4) with $\rho_o = \rho_{o,\,fit}$ for all measured excitation energies.

ρ_o but suppressed in the experimental spectrum at detuned excitation. We can therefore, on the other hand, denote $\rho_{o,\ fit}$ that resulted from the fit to the detuned spectrum as the occupied "dynamic-free" DOS of liquid methanol. This "dynamic-free" DOS is solely based on the electronic states of the free methanol molecule. There is no need for additional states in $\rho_{o,\ fit}$ to account for, e.g., distinct hydrogen bonded structural complexes in the liquid phase.

In Figure 3(c), we depict the results of Eq. (4) for the two approaches for ρ_o together with the experimental data, but now for non-resonant excitation. In this case, the Lorentzian in Eq. (4) has its maximum inside the integration boundaries, and therefore, the unoccupied DOS ρ_u has only minor impact on the resulting spectrum. Consistently, the spectrum resulting from the non-resonant XE spectrum for ρ_o reproduces the experimental data at non-resonant excitation almost fully. The spectrum resulting from the "dynamic-free" DOS $\rho_{o,\ fit}$ is lacking the dominant split peak structure of the experimental spectrum. This confirms our tentative assignment from Sec. III B that the split peak structure is mostly related to nuclear dynamics in the intermediate state.

Finally, we apply Eq. (4) to all measured excitation energies using $\rho_{o,\ fit}$ for the occupied DOS. We compare the results to the experimental data in Figure 3(d). The modeled spectra reproduce the general trend of Raman dispersion up to the resonance position and development of sharp spectral features for excitations above the resonance. However, for excitation energies, where P_{dyn} becomes significant (around 533.7 eV—compare Figure 2(d)), the modeled spectra clearly deviate from the experimental data. Most significant is the fast increase of the spectral component that develops into the low energy split peak component as well as an energy shift of the complete spectrum. For excitations around the O–H σ^* shoulder the intermediate state has anti-bonding character with respect to the O–H bond. This enhances nuclear dynamics and their effect on the RIXS spectra. In addition, screening effects[23,56,57] from the excited electron result in energy shifts (spectator shift) for resonant excitation energies.

D. Normal vs. deuterated methanol

To further investigate the impact of dynamics in the O–H(D) bond on the RIXS spectral profiles, we compare now normal and deuterated methanol (CH_3OH and CD_3OD). For the heavier isotope, these dynamics will be significantly slower.

In Figure 4, we present RIXS spectra of the two methanol forms for three characteristic excitation energies: 535.3 eV (low energy flank), 538.3 eV (absorption maximum), and 549.8 eV (non-resonant). We find a clear difference in the split peak structure between the two isotopes. The low energy component is significantly reduced for deuterated methanol. The remaining spectral features seem to be not sensitive to isotope substitution. This suggests that dynamics in the O–H(D) bond are the main response to the core-excitation and are responsible for formation of the split peak structure.

IV. DISCUSSION

A. Dynamics of the O–H bond and formation of the split peak structure

In this section, we propose a scenario that explains the formation of the split peak structure due to dynamics in the O–H bond of the hydrogen bond donating OH group in the core-excited state.

In Figure 5, we present qualitative one dimensional potential energy curves of a hydrogen bond donating OH group along the O–H $\cdots$ O hydrogen bond coordinate. We depict those states involved in the formation of the split peak structure at non-resonant excitation (ionization): initial ground state, intermediate core-ionized state, and the $2a''$ lone-pair-ionized final state. We limit the discussion here to the $2a''$ lone-pair-ionized final state, since this state gives the biggest contribution to the split peak structure. However, also the $7a'$ ionized final state will contribute to some extent. The potential energy curves in Figure 5 are qualitative in the sense that they are not the result of a quantum mechanical *ab initio* theory. But they are based on the results of extensive calculations for the hydrogen bond donating OH group in the water

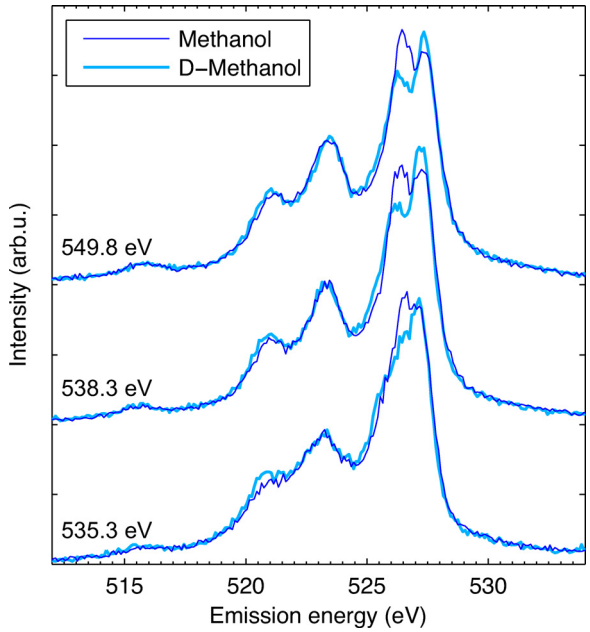

FIG. 4. RIXS spectra of normal and deuterated methanol (D-Methanol) for three characteristic excitation energies.

dimer.[18,58] Quantitatively methanol and water exhibit distinctly different potential energy curves in ground and excited states, especially because of only one hydrogen bond donating OH group in methanol. Yet, the characteristic features of the potentials will be the same for all hydrogen bond donating OH groups, in particular, along the hydrogen bond coordinate. These characteristic features are (see Figure 5): The ground state potential has a single minimum close to the hydrogen bond donating oxygen atom. In the core-ionized state, the potential is repulsive with respect to the initial covalent O–H bond, but bound by the hydrogen bond accepting oxygen atom. The lone-pair-ionized state features a shallow double well potential with a minimum close to each of the oxygen atoms.

Based on these potentials we can understand the formation of the split peak structure as follows: In the core-ionized state, the nuclear wave packet delocalizes between the two oxygen atoms. Hence, the wave packet reaches Franck-Condon overlap with vibrational states in both minima of the lone-pair-ionized final state. Decays into the two minima result in emission at different photon energies. The difference in emission energy depends on the exact shape of the potential and the corresponding vibrational levels. Ljungberg *et al.*[18] applied the full Kramers-Heisenberg scattering formalism (in particular, including interference effects in the scattering process[38,59]) to the quantitatively calculated potentials of the hydrogen bond donating molecule in the water dimer. They found indeed a significant effect on the lone-pair emission line from dynamics in the O–H bond. In their calculations, the vibronic transitions group into two regions separated by about 0.5 eV in emission energy. After adding environmental as well as instrumental broadening, this two peak structure turned into one asymmetric peak for the simple model water dimer. Ljungberg *et al.*[18] interpret the split lone-pair peak in liquid water by the presence of a second peak originating from differently hydrogen bonded species next to the lone-pair peak in liquid water. The asymmetry of the lone-pair peak lifts the second peak, which explains also the isotope effect in liquid water according to these authors.

Ljungberg *et al.*[18] used a comparable short O–O distance of 2.75 Å, as found in water ice to model a typical strong hydrogen bond. Using the O–O distances of liquid methanol as well as including the methyl group in the calculations could increase the asymmetry of the lone-pair emission line more towards a split peak structure as observed in our experimental data. We note that the $7a'$ peak close to the lone-pair peak is lifted in intensity by the asymmetry of the lone-pair peak similar to what Ljungberg *et al.*[18] describe for liquid water. The $7a'$ state

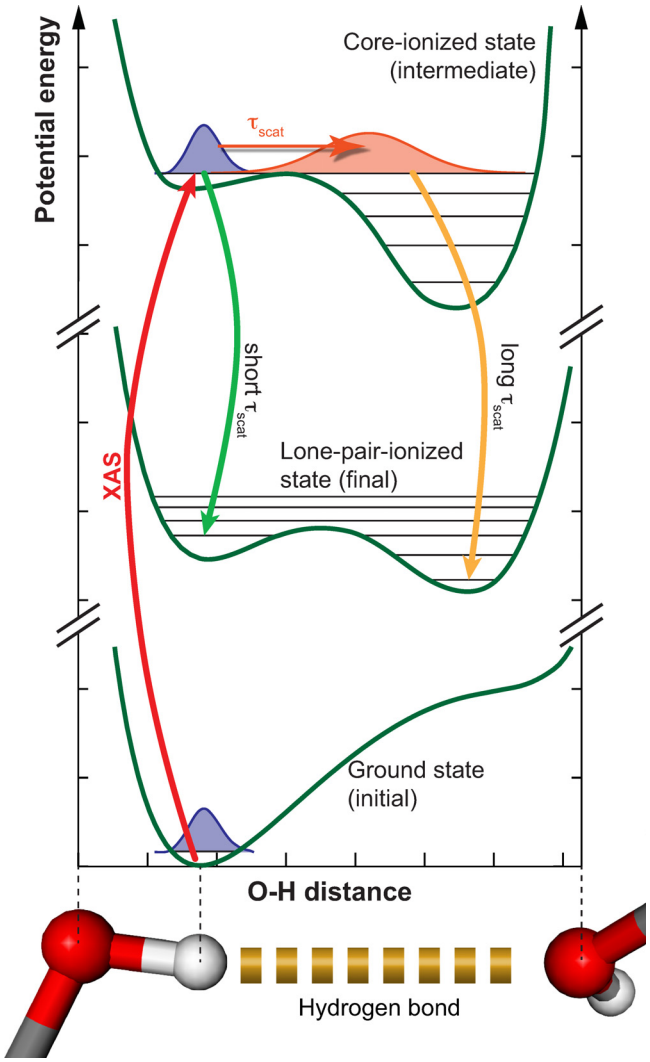

FIG. 5. Proposed mechanism for the formation of the split peak emission feature: Shown are qualitative potential energy curves along the O–H coordinate of a hydrogen bond donating OH group in the ground state, the oxygen 1*s* core-ionized state and the lone-pair-ionized state.

therefore partly contributes to the low energy component of the split peak. However, we can not exclusively assign the low energy component to the $7a'$ state, since for excitation energies between 534.8 and 535.5 eV (see Figures 1 and 2(b)), the $7a'$ state is well resolved next to the two components of the lone-pair peak.

Within the, here, described mechanism, the collapse of the split peak structure into a single emission line when detuning the excitation energy is analog to the collapse of the vibrational progression for decay into the electronic ground state (compare Sec. III B). This narrowing of emission features from electronic excited final states with detuning has been recently described for liquid acetone and isopropanol.[27,35]

B. The effect of hydrogen bonding

The scenario for the formation of the split peak structure described in Sec. IV A applies solely for hydrogen bond donating OH groups, since they just feature the repulsive but bound potential in the core-ionized state and the double well potential in the lone-pair-ionized state. For hydrogen bond accepting or non-hydrogen-bonded OH groups, the scenario will be quite different. Felicíssimo *et al.*[58] have calculated the O–H and O–O potentials of the geometry

optimized water dimer for ionization at the donor and acceptor oxygen site. From the calculated potentials it follows that ionization at the hydrogen bond accepting molecule does not result in significant dynamics in the O–H bond. Instead, the O–O potential is slightly repulsive resulting in a weakening of the hydrogen bond after core level ionization. Similar results have been obtained by Odelius *et al.*[10] For an OH group, that is accepting and donating a hydrogen bond at the same time (as it is the case for most of the molecules in liquid alcohols[28,29]), the situation will be different again. Ultimately changes in the hydrogen bond configuration and strength can influence the dynamics in the core-exited state and hence also affect the split peak structure in RIXS spectra.

To verify this expected influence of the hydrogen bond environment on the RIXS spectral profiles, we compare in Figure 6 RIXS spectra of the linear alcohols from methanol to hexanol in the liquid phase. All alcohols feature a well-resolved split peak structure around 527 eV emission energy for excitation at the absorption maximum (Figure 6(a)) as well as for non-resonant excitation (Figure 6(b)). However, we observe variations in the relative intensities of the two split peak components as a function of carbon chain length. We quantify these variations for both excitation energies in Figure 6(c), where the ratio of the two split peak components (peak heights of the experimental data are divided) is shown as a function of the carbon

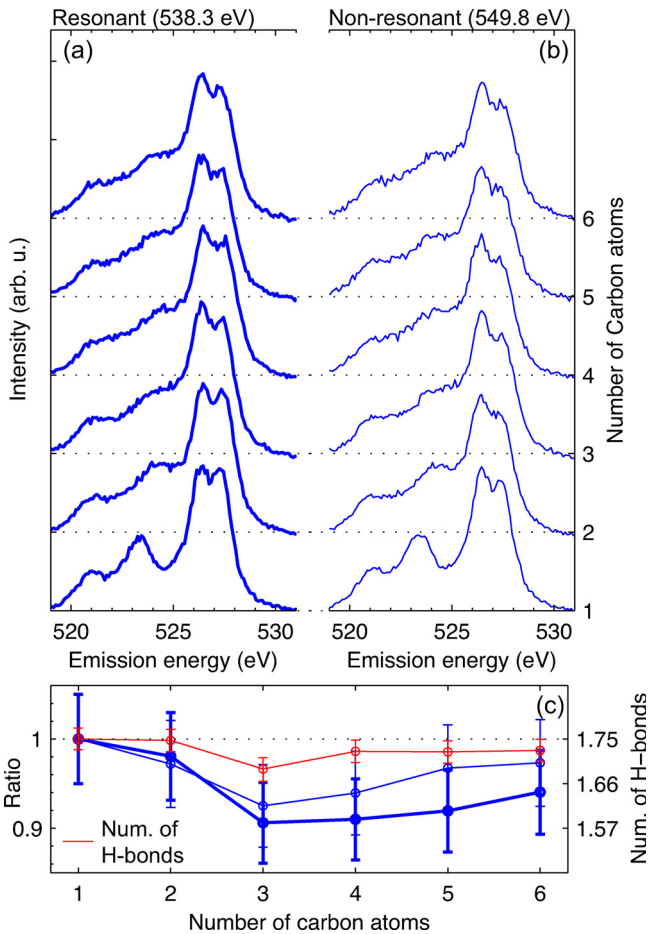

FIG. 6. Impact of the hydrogen bond network on the split peak structure. RIXS spectra for (a) resonant and (b) non-resonant excitation of linear alcohols in the liquid phase with one to six carbon atoms (methanol to hexanol). The spectra are offset for clarity. The corresponding XA spectra measured in total fluorescence yield are shown in the supplementary material[34] (c) Mean number of hydrogen bonds per molecule[29] (red line) as a function carbon chain length together with the ratio of the two split peak components (high-energy/low-energy). Thick and thin blue lines correspond to the ratio at resonant and non-resonant excitation. A description of the error estimate is given in the supplementary material.[34] All values are normalized to the value for methanol (left y-scale). The y-scale on the right gives the number of hydrogen bonds.

chain length. We also include the mean number of hydrogen bonds per molecule in the liquid as determined by Lehtola *et al.*[29] We find a weak but clear correlation between the variation in the split peak intensities and the mean number of hydrogen bonds. In particular, the anomalous behavior of propanol (C_3H_7OH) of having the fewest hydrogen bonds per molecule is also found in the RIXS spectra: The relative intensity of the high emission energy split peak is smallest for propanol.

Accordingly, the split peak structure is also affected by the hydrogen bond environment, even though it has a local molecular origin (dynamics of the O–H bond in the core-excited state). Therefore, we expect that changes in the hydrogen bond environment induced by, e.g., temperature changes also affect the split peak structure.

V. SUMMARY AND CONCLUSIONS

We have performed an experimental RIXS study of liquid methanol in its normal (CH_3OH) and deuterated form (CD_3OD) as well as of the liquid alcohols with longer carbon chains up to hexanol. All liquid alcohols feature a split peak structure in the lone-pair emission region of the non-resonant XE spectrum.

The high quality of the data from liquid methanol in terms of signal-to-noise ratio, spectral resolution, and excitation energy range allowed for a detailed analysis of the vibrational progression of the decay into the electronic ground state and the connected nuclear dynamics in the intermediate core-excited state.

We determined the characteristic time in the core-excited state until nuclear dynamics give a measurable contribution to the RIXS spectral profiles to $\tau_{dyn} = 1.2 \pm 0.8$ fs for liquid methanol. By detuning the excitation energy from the absorption resonance, we reduced the effective scattering time well below τ_{dyn} and hereby suppressed nuclear dynamics in the RIXS process to a minimum.

From the RIXS spectra at strong detuning we retrieved the "dynamic-free" local partial DOS of liquid methanol. The "dynamic-free" DOS is fully described by the electronic states of the free methanol molecule and it features, in particular, no split peak structure in the lone-pair region. This, together with the comparison of normal and deuterated methanol gave evidence that the split peak structure in liquid alcohols originates from dynamics in the O–H bond in the core-excited state.

We proposed a mechanism for the formation of the split peak structure that is based on qualitative potential energy curves of the hydrogen bond donating OH group in the core- and lone-pair-ionized state. In this picture, the splitting originates from the local dynamics of the O–H bond in the core-excited state. At the same time, we showed that the splitting is also sensitive to changes in the hydrogen bond network since the specific hydrogen bond configuration has influence on the O–H bond dynamics.

We conclude that the split peak structure in RIXS spectra from liquid alcohols originates from local dynamics of the O–H bond in the core-excited state of hydrogen bond donating OH groups. The splitting is not a signature of distinct structural motifs in the liquid alcohols. This finding is at variance with the study of Kashtanov *et al.*,[26] where the two split components in the lone-pair region have been assigned to hydrogen bonded rings and chains, respectively. However, we note that our analysis does not exclude the existence of different structural motifs.

Our findings contribute to a better understanding of local molecular, dynamical, as well as structural contributions in RIXS from the liquid phase. We expect that the detuning approach and the retrieval of the "dynamic-free" DOS will find broader application in the investigation of complex molecular and liquid systems.

ACKNOWLEDGMENTS

We are grateful to the Institute for Nanometer Optics and Technology at the Helmholtz-Zentrum Berlin and to Christian Weniger for manufacturing the silicon based sample cells for the transmission measurements. Continuous assistance of the BESSY II staff is acknowledged. Furthermore, we thank Henning Schröder for his support during the measurements.

[1]J. Stöhr, *NEXAFS Spectroscopy* (Springer Verlag, 1992).
[2]F. de Groot and A. Kotani, *Core Level Spectroscopy of Solids* (CRC Press, 2008).
[3]A. Nilsson and L. G. M. Petterson, "Adsorbate electronic structure and bonding on metal surfaces," in *Chemical Bonding at Surfaces and Interfaces*, edited by A. Nilsson, L. G. M. Petterson, and J. K. Nørskov (Elsevier B. V., 2008).
[4]P. Wernet, D. Nordlund, U. Bergmann, M. Cavalleri, M. Odelius, H. Ogasawara, L.-Å. Näslund, T. K. Hirsch, L. Ojamäe, P. Glatzel, L. G. M. Pettersson, and A. Nilsson, "The structure of the first coordination shell in liquid water," Science **304**, 995–999 (2004).
[5]J. D. Smith, C. D. Cappa, K. R. Wilson, B. M. Messer, R. C. Cohen, and R. J. Saykally, "Energetics of hydrogen bond network rearrangements in liquid water," Science **306**, 851–853 (2004).
[6]A. Nilsson, D. Nordlund, I. Waluyo, N. Huang, H. Ogasawara, S. Kaya, U. Bergmann, L.-Å. Näslund, H. Öström, P. Wernet, K. Andersson, T. Schiros, and L. G. M. Pettersson, "X-ray absorption spectroscopy and X-ray Raman scattering of water and ice; an experimental view," J. Electron Spectrosc. Relat. Phenom. **177**, 99–129 (2010).
[7]B. Winter, U. Hergenhahn, M. Faubel, O. Björneholm, and I. V. Hertel, "Hydrogen bonding in liquid water probed by resonant Auger-electron spectroscopy," J. Chem. Phys. **127**, 094501 (2007).
[8]D. Nordlund, H. Ogasawara, H. Bluhm, O. Takahashi, M. Odelius, M. Nagasono, L. G. M. Pettersson, and A. Nilsson, "Probing the electron delocalization in liquid water and ice at attosecond time scales," Phys. Rev. Lett. **99**, 217406 (2007).
[9]J.-H. Guo, Y. Luo, A. Augustsson, J.-E. Rubensson, C. Såthe, H. Ågren, H. Siegbahn, and J. Nordgren, "X-Ray emission spectroscopy of hydrogen bonding and electronic structure of liquid water," Phys. Rev. Lett. **89**, 137402 (2002).
[10]M. Odelius, H. Ogasawara, D. Nordlund, O. Fuchs, L. Weinhardt, F. Maier, E. Umbach, C. Heske, Y. Zubavichus, M. Grunze, J. Denlinger, L. G. M. Pettersson, and A. Nilsson, "Ultrafast core-hole-induced dynamics in water probed by x-ray emission spectroscopy," Phys. Rev. Lett. **94**, 227401 (2005).
[11]T. Tokushima, Y. Harada, O. Takahashi, Y. Senba, H. Ohashi, L. G. M. Pettersson, A. Nilsson, and S. Shin, "High resolution x-ray emission spectroscopy of liquid water: The observation of two structural motifs," Chem. Phys. Lett. **460**, 387–400 (2008).
[12]O. Fuchs, M. Zharnikov, L. Weinhardt, M. Blum, M. Weigand, Y. Zubavichus, M. Bär, F. Maier, J. Denlinger, C. Heske, M. Grunze, and E. Umbach, "Isotope and temperature effects in liquid water probed by x-ray absorption and resonant x-ray emission spectroscopy," Phys. Rev. Lett. **100**, 027801 (2008).
[13]K. M. Lange, R. Könnecke, S. Ghadimi, R. Golnak, M. A. Soldatov, K. F. Hodeck, A. Soldatov, and E. F. Aziz, "High resolution x-ray emission spectroscopy of water and aqueous ions using the micro-jet technique," Chem. Phys. **377**, 1–5 (2010).
[14]A. Nilsson, T. Tokushima, Y. Horikawa, Y. Harada, M. P. Ljungberg, S. Shin, and L. G. M. Pettersson, "Resonant inelastic x-ray scattering of liquid water," J. Electron Spectrosc. Relat. Phenom. **188**, 84–100 (2013).
[15]Y. Harada, T. Tokushima, Y. Horikawa, O. Takahashi, H. Niwa, M. Kobayashi, M. Oshima, Y. Senba, H. Ohashi, K. T. Wikfeldt, A. Nilsson, L. G. M. Pettersson, and S. Shin, "Selective probing of the OH or OD stretch vibration in liquid water using resonant inelastic soft-x-ray scattering," Phys. Rev. Lett. **111**, 193001 (2013).
[16]M. Odelius, "Molecular dynamics simulations of fine structure in oxygen K-edge x-ray emission spectra of liquid water and ice," Phys. Rev. B **79**, 144204 (2009).
[17]M. Odelius, "Information content in O[1s] K-edge x-ray emission spectroscopy of liquid water," J. Phys. Chem. A **113**, 8176–8181 (2009).
[18]M. P. Ljungberg, L. G. M. Pettersson, and A. Nilsson, "Vibrational interference effects in x-ray emission of a model water dimer: Implications for the interpretation of the liquid spectrum," J. Chem. Phys. **134**, 044513 (2011).
[19]L. G. M. Pettersson, T. Tokushima, Y. Harada, O. Takahashi, S. Shin, and A. Nilsson, "Comment on 'Isotope and temperature effects in liquid water probed by x-ray absorption and resonant x-ray emission spectroscopy,'" Phys. Rev. Lett. **100**, 249801 (2008).
[20]O. Fuchs, M. Zharnikov, L. Weinhardt, M. Blum, M. Weigand, Y. Zubavichus, M. Bär, F. Maier, J. Denlinger, C. Heske, M. Grunze, and E. Umbach, "Fuchs *et al*. Reply:," Phys. Rev. Lett. **100**, 249802 (2008).
[21]J. Forsberg, J. Gråsjö, B. Brena, J. Nordgren, L.-C. Duda, and J.-E. Rubensson, "Angular anisotropy of resonant inelastic soft x-ray scattering from liquid water," Phys. Rev. B **79**, 132203 (2009).
[22]K. M. Lange, M. Soldatov, R. Golnak, M. Gotz, N. Engel, R. Könnecke, J.-E. Rubensson, and E. F. Aziz, "X-ray emission from pure and dilute H_2O and D_2O in a liquid microjet: Hydrogen bonds and nuclear dynamics," Phys. Rev. B **85**, 155104 (2012).
[23]L. Weinhardt, A. Benkert, F. Meyer, M. Blum, R. G. Wilks, W. Yang, M. Bär, F. Reinert, and C. Heske, "Nuclear dynamics and spectator effects in resonant inelastic soft x-ray scattering of gas-phase water molecules," J. Chem. Phys. **136**, 144311 (2012).
[24]J.-H. Guo, Y. Luo, A. Augustsson, S. Kashtanov, J.-E. Rubensson, D. K. Shuh, H. Ågren, and J. Nordgren, "Molecular structure of alcohol-water mixtures," Phys. Rev. Lett. **91**, 157401 (2003).
[25]J.-H. Guo, Y. Luo, A. Augustsson, S. Kashtanov, J.-E. Rubensson, D. Shuh, V. Zhuang, P. Ross, H. Ågren, and J. Nordgren, "The molecular structure of alcohol-water mixtures determined by soft-x-ray absorption and emission spectroscopy," J. Electron Spectrosc. Relat. Phenom. **137–140**, 425–428 (2004).
[26]S. Kashtanov, A. Augustson, J.-E. Rubensson, J. Nordgren, H. Ågren, J.-H. Guo, and Y. Luo, "Chemical and electronic structures of liquid methanol from x-ray emission spectroscopy and density functional theory," Phys. Rev. B **71**, 104205 (2005).
[27]Schreck *et al*., "Local valence electronic structure and extended potential energy surfaces of the hydrogen and covalent O-H bond from vibrational resolved resonant inelastic x-ray scattering," Phys. Rev. B (to be submitted).
[28]M. Tomšič, A. Jamnik, G. Fritz-Popovski, O. Glatter, and L. Vlček, "Structural properties of pure simple alcohols from ethanol, propanol, butanol, pentanol, to hexanol: Comparing Monte Carlo simulations with experimental SAXS data," J. Phys. Chem. B **111**, 1738–1751 (2007).
[29]J. Lehtola, M. Hakala, and K. Hämäläinen, "Structure of liquid linear alcohols," J. Phys. Chem. B **114**, 6426–6436 (2010).
[30]F. Gel'mukhanov and H. Ågren, "Resonant x-ray Raman scattering," Phys. Rep. **312**, 87–330 (1999).

[31]S. Schreck, G. Gavrila, C. Weniger, and P. Wernet, "A sample holder for soft x-ray absorption spectroscopy of liquids in transmission mode," Rev. Sci. Instrum. **82**, 103101 (2011).
[32]K. Kunnus, I. Rajkovic, S. Schreck, W. Quevedo, S. Eckert, M. Beye, E. Suljoti, C. Weniger, C. Kalus, S. Grübel, M. Scholz, D. Nordlund, W. Zhang, R. W. Hartsock, K. J. Gaffney, W. F. Schlotter, J. J. Turner, B. Kennedy, F. Hennies, S. Techert, P. Wernet, and A. Föhlisch, "A setup for resonant inelastic soft x-ray scattering on liquids at free electron laser light sources," Rev. Sci. Instrum. **83**, 123109 (2012).
[33]K. R. Wilson, M. Cavalleri, B. S. Rude, R. D. Schaller, T. Catalano, A. Nilsson, R. J. Saykally, and L. G. M. Pettersson, "X-ray absorption spectroscopy of liquid methanol microjets: Bulk electronic structure and hydrogen bonding network," J. Phys. Chem. B **109**, 10194–10203 (2005).
[34]See supplementary material at http://dx.doi.org/10.1063/1.4897981 for the description of the interpolation of the high-energy tail of decay into electronic excited states in Figure 2(c), a discussion of the uncertainties and error bars in Figures 2 and 6, the alignment of the DOS in Eq. (4), details on the spectrum calculations for the methanol molecule and the TFY XA spectra of the linear alcohols.
[35]Y.-P. Sun, F. Hennies, A. Pietzsch, B. Kennedy, T. Schmitt, V. N. Strocov, J. Andersson, M. Berglund, J.-E. Rubensson, K. Aidas, F. Gel'mukhanov, M. Odelius, and A. Föhlisch, "Intramolecular soft modes and intermolecular interactions in liquid acetone," Phys. Rev. B **84**, 132202 (2011).
[36]F. Gel'mukhanov, T. Privalov, and H. Ågren, "Collapse of vibrational structure in spectra of resonant x-ray Raman scattering," Phys. Rev. A **56**, 256–264 (1997).
[37]M. Neeb, J.-E. Rubensson, M. Biermann, and W. Eberhardt, "Coherent excitation of vibrational wave functions observed in core hole decay spectra of O_2, N_2, and CO," J. Electron Spectrosc. Relat. Phenom. **67**, 261–274 (1994).
[38]F. Gel'mukhanov, H. Ågren, M. Neeb, J.-E. Rubensson, and A. Bringer, "Integral properties of channel interference in resonant x-ray scattering," Phys. Lett. A **211**, 101–108 (1996).
[39]O. Björneholm, A. Nilsson, A. Sandell, B. Hernnäs, and N. Mårtensson, "Determination of time scales for charge-transfer screening in physisorbed molecules," Phys. Rev. Lett. **68**, 1892–1895 (1992).
[40]A. Naves de Brito, A. Naves de Brito, O. Björneholm, J. S. Neto, A. Machado, S. Svensson, A. Ausmees, S. J. Osborne, L. J. Sæthre, H. Aksela, O.-P. Sairanen, A. Kivimäki, E. Nõmmiste, and S. Aksela, "Fast dissociation of resonantly core excited H_2S studied by vibrational and temporal analysis of the Auger spectra," J. Mol. Struct.: THEOCHEM **394**, 135–145 (1997).
[41]P. A. Brühwiler, O. Karis, and N. Mårtensson, "Charge-transfer dynamics studied using resonant core spectroscopies," Rev. Mod. Phys. **74**, 703–740 (2002).
[42]I. Hjelte, M. Piancastelli, C. Jansson, K. Wiesner, O. Björneholm, M. Bässler, S. Sorensen, and S. Svensson, "Evidence of ultra-fast dissociation in ammonia observed by resonant Auger electron spectroscopy," Chem. Phys. Lett. **370**, 781–788 (2003).
[43]J.-E. Rubensson, "RIXS dynamics for beginners," J. Electron Spectrosc. Relat. Phenom. **110–111**, 135–151 (2000).
[44]J. Tulkki and T. Åberg, "Statistical theory of electronic Raman resonance scattering by oriented atoms," J. Phys. B: At. Mol. Phys. **13**, 3341–3360 (1980).
[45]J. Tulkki and T. Åberg, "Behaviour of Raman resonance scattering across the K x-ray absorption edge," J. Phys. B: At. Mol. Phys. **15**, L435–L440 (1982).
[46]J. Jiménez-Mier, J. van Ek, D. Ederer, T. Callcott, J. Jia, J. Carlisle, L. Terminello, A. Asfaw, and R. Perera, "Dynamical behavior of x-ray absorption and scattering at the L edge of titanium compounds: Experiment and theory," Phys. Rev. B **59**, 2649–2658 (1999).
[47]P. L. Cowan, "Resonant x-ray Raman scattering from atoms and molecules," in *Resonant Anomalous X-Ray Scattering: Theory and Applications*, edited by G. Materlik, C. J. Sparks, and K. Fischer (North-Holland, Amsterdam, 1994).
[48]J. J. Kas, J. J. Rehr, J. A. Soininen, and P. Glatzel, "Real-space Green's function approach to resonant inelastic x-ray scattering," Phys. Rev. B **83**, 235114 (2011).
[49]M. Magnuson, J.-E. Rubensson, A. Föhlisch, N. Wassdahl, A. Nilsson, and N. Mårtensson, "X-ray fluorescence spectra of metals excited below threshold," Phys. Rev. B **68**, 045119 (2003).
[50]H. Hayashi, R. Takeda, Y. Udagawa, T. Nakamura, H. Miyagawa, H. Shoji, S. Nanao, and N. Kawamura, "Lifetime-broadening-suppressed/free XANES spectroscopy by high-resolution resonant inelastic x-ray scattering," Phys. Rev. B **68**, 045122 (2003).
[51]H. Hayashi, "Lifetime-broadening-suppressed selective XAFS spectroscopy," Anal. Sci. **24**, 15–23 (2008).
[52]J. Szlachetko, D. Ferri, V. Marchionni, A. Kambolis, O. V. Safonova, C. J. Milne, O. Kröcher, M. Nachtegaal, and J. Sá, "Subsecond and *in situ* chemical speciation of Pt/Al_2O_3 during oxidation-reduction cycles monitored by high-energy resolution off-resonant X-ray spectroscopy," J. Am. Chem. Soc. **135**, 19071–19074 (2013).
[53]J. Szlachetko, C. J. Milne, J. Hoszowska, J.-C. Dousse, W. Błachucki, J. Sà, Y. Kayser, M. Messerschmidt, R. Abela, S. Boutet, C. David, G. Williams, M. Pajek, B. D. Patterson, G. Smolentsev, J. A. van Bokhoven, and M. Nachtegaal, "Communication: The electronic structure of matter probed with a single femtosecond hard x-ray pulse," Struct. Dyn. **1**, 021101 (2014).
[54]C. Glover, T. Schmitt, M. Mattesini, M. Adell, L. Ilver, J. Kanski, L. Kjeldgaard, M. Agåker, N. Mårtensson, R. Ahuja, J. Nordgren, and J.-E. Rubensson, "Stationary and dispersive features in resonant inelastic soft X-ray scattering at the Ge 3p resonances," J. Electron Spectrosc. Relat. Phenom. **173**, 103–107 (2009).
[55]A. Nilsson and N. Mårtensson, "Initial and final state rules in x-ray spectroscopies of adsorbates," Physica B **208–209**, 19–22 (1995).
[56]H. Ågren, Y. Luo, F. Gel'mukhanov, and H. J. A. Jensen, "Screening in resonant x-ray emission of molecules," J. Electron Spectrosc. Relat. Phenom. **82**, 125–134 (1996).
[57]P. Skytt, P. Glans, K. Gunnelin, J. Guo, J. Nordgren, Y. Luo, and H. Ågren, "Role of screening and angular distributions in resonant x-ray emission of CO," Phys. Rev. A **55**, 134–145 (1997).
[58]V. Felicíssimo, I. Minkov, F. Guimarães, F. Gel'mukhanov, A. Cesar, and H. Ågren, "A theoretical study of the role of the hydrogen bond on core ionization of the water dimer," Chem. Phys. **312**, 311–318 (2005).
[59]F. Gel'mukhanov, L. Mazalov, and A. Kondratenko, "A theory of vibrational structure in the x-ray spectra of molecules," Chem. Phys. Lett. **46**, 133–137 (1977).